Two experimental instruments inspired by radio technologies

Marinos Koutsomichalis
Cyprus Univ. of Technology
30 Arch. Kyprianou, 3036
Limassol, Cyprus
m.koutsomichalis@cut.ac.cy

ABSTRACT

This short paper accounts for (a) a wearable radio receiver that can be operated in the fashion of a monochord string instrument, and (b) for a rotating induction coil. Technical aspects are discussed and the process is exposed as laboratory experimentation with radio technologies.

Author Keywords

Radio, VLF, Electronics, Critical Design, NIME

CCS Concepts

•**Hardware** → **Signal processing systems; Sound-based input / output;** *Electro-mechanical devices;*

1. BACKGROUND

The earliest instances of radio-inspired NIME are most likely the *Radiopiano* and the *Radiotone* that are referenced in [10] as being already in use on 1931. *Radiotone* is also a NIME by Sancristoforo[1] that employs X-Rays and a cosmic ray detector to control music tones. Controlling music performance is also the focus with the various *Radio batons*, wherein radio technology is utilized to extrapolate the 3D positioning of a stick [2]. Another continuum is concerned with environmental radio-scapes. Kubisch designs instruments that allow audiences to listen to transmitted or environmental radio signals since the 1970s. [6]. In Bowers' *Ghost Radio*, demodulated radio signals control a modular synthesizer[1]. Miyazaki's *Detector* allows us to listen to (the otherwise inaudible) condition of 'wirelessness'[7]. Hinterding's graphite-based drawings afford the reception of VLF signals and their playful performance[3, p. 38–39]. Other approaches zoom in the ways in which radio signals resonate the biosphere. An Apo33 exhibition[2] zooms in radio *vis-á-vis* mycelia networks, trees, and plants while *Radio Mycelium* pivots on fungal mycelia[8].

[1]`https://blog.bela.io/radiotone-x-ray-synthesizer` Accessed Feb 7, 2024
[2]`https://apo33.org/?p=9480` Accessed Feb 7, 2024

NIME'24, 4–6 September, Utrecht, The Netherlands.

Figure 1: ***Antenna mono-chord.***

2. ANTENNA MONO-CHORD

Antenna mono-chord is a radio receiver capable of FM and two distinct SW bands that can be 'performed' in a string instrument like fashion. Rather than being the product of some structured ideation or design process, *Antenna mono-chord* has surfaced experimentation with haphazard materials lying around at the author's studio and, as such, it should be rather thought of as "*a record of its own making*"[5]. It follows the affordancies of a long 'soft-pot' slider; it naturally found its place on a piece of wood and, given the author's long lasting interest in radio technologies and his ongoing experiments at that time with *Roto-ctor*, the idea of a radio receiver controlled by the former suggested itself immediately.

The circuity is scavenged from a commercial apparatus and subsequently tinkered with accordingly so that the soft-pot controls its tuning and so that one may switch between FM/SW bands via a pair of momentary lapse push-buttons. The soft-pot is where one would expect to find a string in a monochord instrument while the latter are where one would typically pluck it. The instrument also features a long telescopic antenna on the side, a speaker and a line-out TS jack on the other, a battery holder and a switch to toggle between speaker/line output on the back, and a leather stripe mounted on steel hooks at the top. Components have been glued onto the long piece of wood using mostly two-part polyurethane adhesive and, on a few occasions, two-part epoxy stucco. Photos 1 and 2 illustrate the resulting instrument.

3. ROTO-CTOR

Roto-ctor is inspired by Romero *et al.* inductor for ELF/VLF monitoring[11]. Given that inductors are directional sensors, electro-mechanical rotation (akin to that of radars) suggests itself for interesting phasing effects. Such a device would also radiate over short distances. The eventual

Figure 2: *Antenna mono-chord*; detail.

instrument features:

- a ferrite core induction coil
- an electro-mechanical system to achieve full rotation over 360°
- a motor-driver controlling the rotation speed
- a line-level pre-amplifier
- transmitting circuity (in the same enclosure as above)
- a footswitch to switch between RX/TX operation

The inductor's core comprises a series of seven $\Phi 10\,\mathrm{mm}/L$ $10\,\mathrm{cm}$ ferroxcube type 3C90 ferrite rods. The manufacturer ratings suggest an average permeability of $\mu_i = 2300 \pm 20\%$ at frequencies $f \leqslant 10\,\mathrm{KHz}$; it needs be emphasized that $\mu_i \propto f$. As shown in Fig. 3, the rods are enclosed in shrinking tube and a plastic pipe; then wrapped with $6.5\,\mathrm{Km}$ of $\Phi 0.08\,\mathrm{mm}$ enamel copper wire; then more shrinking tube, a slotted copper tube as a shield, bubble wrap, and eventually a hard plastic tube. Thus, the resulting device is protected from dust, liquids, physical stress, and transversal current loops.

Rotating the inductor is a rather challenging affair in a DIY context. The industrial grade through-bearing slip-ring shown in Fig. 4 is used to achieve seamless rotation without twisting any cables. A motor of appropriate characteristics is selected and fastened to a stand. Motor motion needs be transferred to the inductor in a safe, stable, and balanced manner. After trial and error, the author attacked the problem in this fashion: the supporting brace is mounted onto a $M10$ threaded rod going through the slip-ring and glued half the way into a coupling nut. Three

Figure 3: Preparing the induction coil.

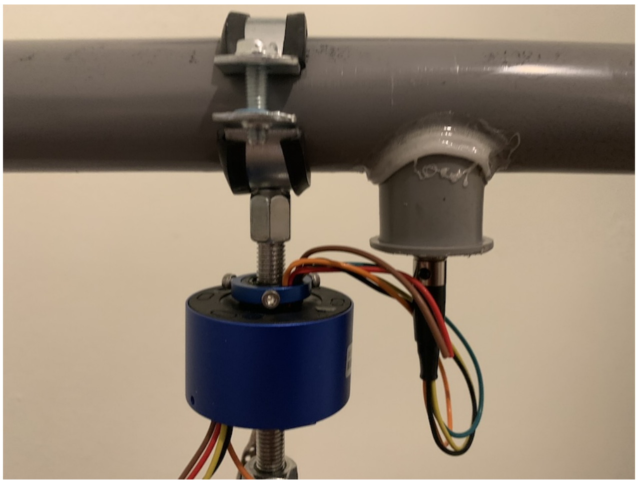

Figure 4: Roto-ctor; detail.

Figure 5: Creating a threaded coupler from scratch.

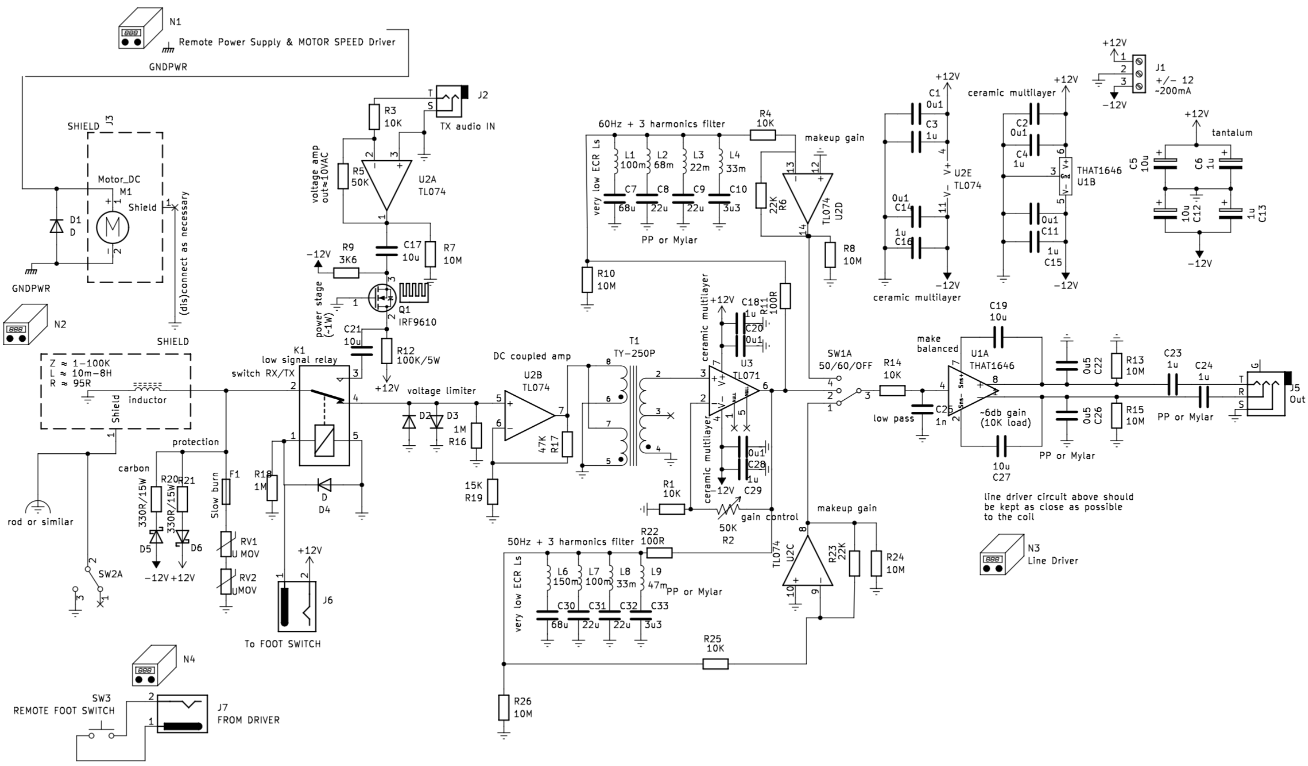

Figure 6: ***Roto-ctor*** **schematics**

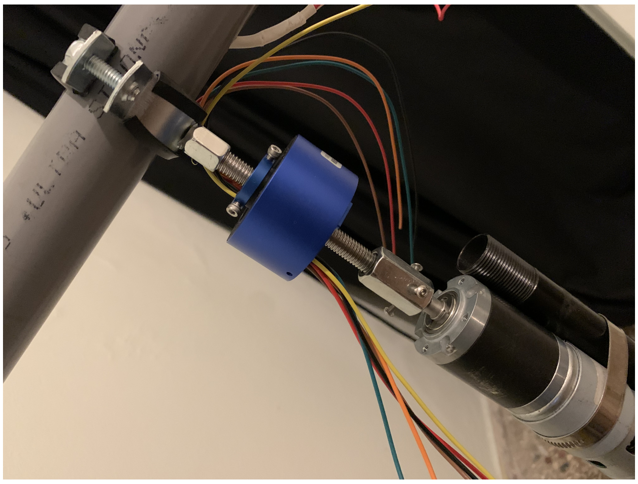

Figure 7: Roto-ctor; detail.

equidistant threaded holes are opened to the other side of this coupler that goes over the motor shaft. It is then possible to employ small screws to eliminate micro-lateral inclinations so as to keep everything firm and centered.

The motor-driver comprises a 1 A/12 V switching power supply and a ready-made component driver. A diode is used to protect the motor from back-EMF. Note that the motor will induce its own electromagnetic signals; while this aids to the particular character of the instrument, it needs be controlled. Accordingly, a grounded metallic mesh is wrapped around the motor so as to filter out most of the produced static.

RX/TX circuity are designed and implemented directly on a perforating board stage by stage, in a process of on-the-fly experimentation, trial/error, testing, and measuring. The eventual schematic is shown in Fig. 6. It requires a linear power supply of 12 VAV/200 mA. The inductor is measured to have a resistive impedance component $R_L \approx 95\,\Omega$ and a non-linear reactant one that is illustrated in Fig. 8 (this is due to parasitic capacitance and because $\mu_i \propto f$). The inductance L is then a function of frequency f so that for $\psi \equiv fL(f)$, the total impedance is

$$Z_L \equiv R_L + X_L = R_L + 2\pi f\psi \implies$$

$$Z_L = \zeta(\psi) = (95 + 2\pi\psi)\Omega \tag{1}$$

It is decided to focus on the $[0.5, 4]$KHz region where it is measured that $6\,\text{H} \leqslant L \leqslant 8\,\text{H}$ so that $1\,\text{KHz} \times 6\,\text{H} \leqslant \psi \leqslant 2\,\text{KHz} \times 8\,\text{H}$. The circuit is then optimized for an average impedance of

$$\begin{aligned}\bar{Z}_L &= \frac{1}{(8\times 2000) - (6\times 1000)} \int_{6\times 1000}^{8\times 2000} \zeta(\psi) \\ &= \frac{1}{10000}\int_{6000}^{16000} \zeta(\psi) = \frac{1}{10}\int_{6}^{16} \zeta(1000\psi) \\ &\overset{Eq.1}{=} \frac{1}{10}\int_{6}^{16} (95 + 2000\pi\psi) \\ &= \frac{1}{10}\left(95\psi\Big|_6^{16} + 2000\pi\frac{\psi^2}{2}\Big|_6^{16}\right) \approx 70\,\text{K}\Omega\end{aligned}$$

Looking out of the inductor one finds two parallel back-EMF protection stages. A couple of ‘snubber’ Schottky/Resistor pairs in parallel provide a low impedance path to the AC ground. With the intended power supply of 200 mA and since $Q1$ is in a unity-gain configuration, the maximum

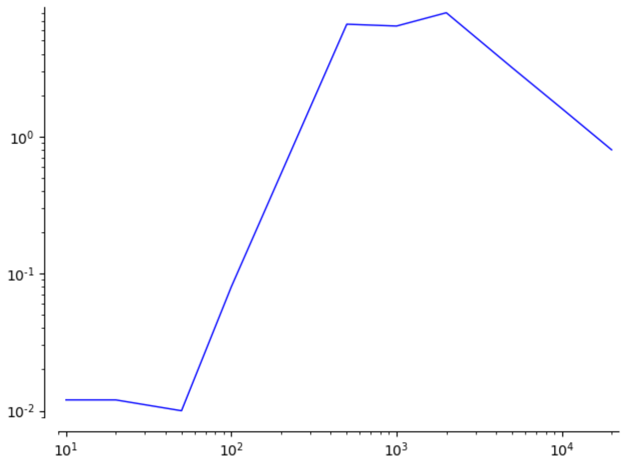

Figure 8: Frequency (x-axis) vs Inductance plot (logarithmic).

energy is $\frac{L_{\triangle} I^2}{2} = 0.16\,\text{J}$; for a 1 ms transient, this amounts to $\frac{0.16\,\text{J}}{0.01\,\text{s}} = 16\,\text{W}$ of power. Accordingly, $R_{20/21}$ are rated for 15 W while $D_{5/6}$ (and all related cabling) are rated for at least 500 mA. The second protection stage comprises two MOVs rated at 18 VAC and a slow-burn fuse rated at 400 mA (since MOVs eventually fail with time).

A remote footswitch controls the relay switching TX/RX. The TX stage is rather straightforward; just a MOSFET Q_1 in a common-gate configuration. Output impedance is approximated by [12, 4.41–4.42]

$$Z_O \approx r_o(g_m R_S + 1)||R_D \tag{2}$$

IRF9610 datasheet gives $I_D > 2.5\,\text{A}$ for $V_{DS} > 24\,\text{V}$ and $V_{GS} \approx 12\,\text{V}$[13]. In real-life, however, I_D is limited to what the power supply can offer and this should be 200 mA (and in any case no more than 400 mA) here. Accordingly,

$$r_o = \frac{\partial V_{DS}}{\partial I_D} \approx \frac{V_{DS}}{I_D} \approx \frac{24V}{0.2A} \approx 120\,\Omega$$

According to[13], $g_m \approx 0.5\,\text{S}$ for $I_D \approx 0.2\,\text{A}$. Then, for $R_D = R_{12} = 100\,\text{K}\Omega$ and $R_S = R_9 = 3.6\,\text{K}\Omega$

$$Z_O \overset{Eq.2}{\approx} 120(0.5 \times 3.6\,\text{K}\Omega + 1)||100\,\text{K}\Omega \approx 70\,\text{K}\Omega$$

so that $Z_O = \bar{Z}_L$ and so that maximum power transfer is guaranteed.

First in the RX pipeline comes the $D_2||D_3$ pair that limits the input signal roughly between $\pm 700\,\text{mV}$. A three stage amplification network comes next. It is desired to use an audio transformer (T_1) in this circuit for its excellent DC-blocking characteristics and to provide complete electronic isolation between the inductor and audio output. The signal is too weak to directly drive T_1 however, so that it first passes through a DC-coupled non-inverting amplification stage with gain $g = 1 + \frac{R_{17}}{R_{19}} = 1 + \frac{47\,\text{K}\Omega}{15\,\text{K}\Omega} \approx 4$. T_1 in a $1:2$ configuration provides an additional voltage gain of $g = 4$. Finally, another non-inverting amplifier with gain control provides up to $1 + \frac{R_2}{R_1} = 1 + \frac{50\,\text{K}\Omega}{10\,\text{K}\Omega} = 6$ gain (when the signal is very weak). The signal is then split and sent to two different filter banks. Via a mechanical switch the unfiltered signal or the output of either of the two filter banks is selected and, eventually converted to a balanced line signal by means of a THAT1646 IC.

The filters have an identical topology of four series LC

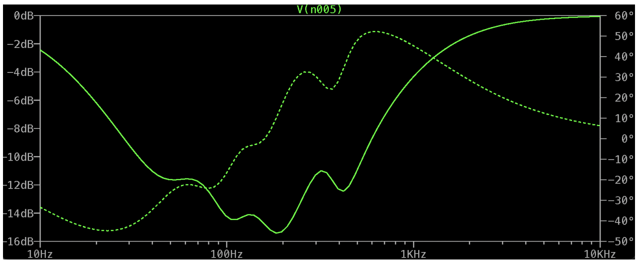

Figure 9: *Roto-ctor* 50 Hz and overtones filter bank frequency response (logarithmic)

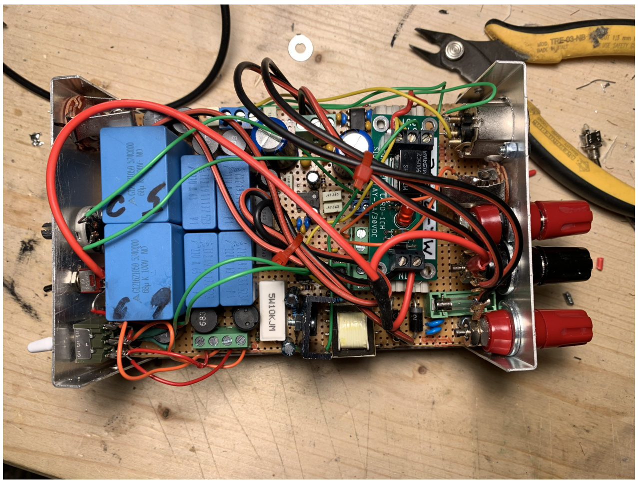

Figure 10: Roto-ctor circuity

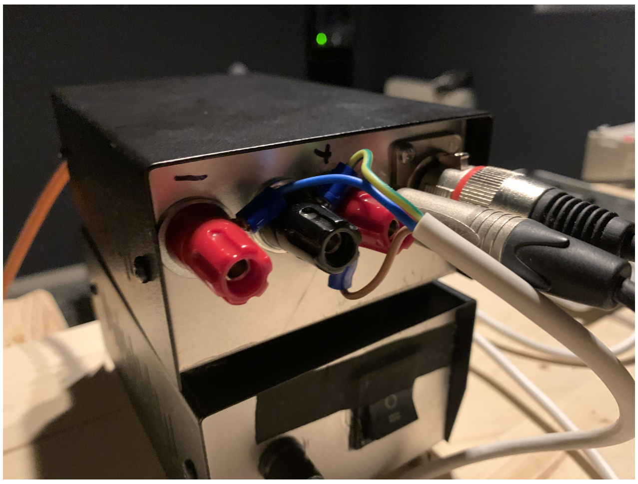

Figure 11: Roto-ctor motor driver and TX/RX amplifier

Figure 12: Roto-ctor in motion;

tanks in parallel and an inverting amplifier with $g = \frac{R_{6/23}}{R_{4/25}} = \frac{22\,\mathrm{K\Omega}}{10\,\mathrm{K\Omega}} = 2.2$ to make-up for the lost gain. The filter banks comprise 4 individual notch filters each with their resonant frequencies at a 50 Hz and 60 Hz fundamental, respectively, and three overtone harmonics, so that electrical hum can be filtered worldwide. Note that the bandwidth of the notches is directly proportion to the coils' ESR, so that coils with exceptionally low ESR are necessary. Figure 9 illustrates the resulting frequency response for the 50 Hz filter, also taking into account the measured ESR.

4. FUTURE WORK

The author is currently finalizing *Vorticular Radio*, *i.e.* an experimental radio receiver utilizing the rudimentary parts of an early 20th century radio receiver (DIY variable capacitors and coils, mineral crystal detector) and intentionally unstable electronic circuit.

5. REFERENCES

[1] J. Bowers, J. Richards, T. Shaw, J. Frize, B. Freeth, S. Topley, N. Spowage, S. Jones, A. Patel, R. Li, et al. One knob to rule them all: reductionist interfaces for expansionist research. In *New Interfaces For Musical Expression*. Newcastle University, 2016.

[2] R. Bresin, K. F. Hansen, and S. Dahl. The radio baton as configurable musical instrument and controller. In *Proceedings of the Stockholm Music Acoustics Conference*, pages 689–691, 2003.

[3] J. L. de Vicente, H. Harger, and J. Perelló. *Invisible fields: geographies of radio waves*. ACTAR Publishers, 2011.

[4] Ferroxcube. *3C90 Material Specification*, 2004.

[5] M. Koutsomichalis. Instruments that are more than instruments (and other stories). *Ricercare*, 2022.

[6] A. Licht. Sound art: Origins, development and ambiguities. *Organised Sound*, 14(1):3–10, 2009.

[7] S. Miyazaki. Urban sounds unheard-of: a media archaeology of ubiquitous infospheres. *Continuum*, 27(4):514–522, 2013.

[8] A. Pomyalova. Radio mycelium (2018)–eine jam session mit pilzen? *Transpositiones*, 1(1):119–136, 2022.

[9] J. C. D. Regino. Parasitic radio: combining fm radio signals with environmental sensor data via computing techniques for soundscape creation. *Politics of the Machine Beirut 2019 2*, pages 37–40, 2019.

[10] C. Roads. Early electronic music instruments: Time line 1899-1950. *Computer Music Journal*, 20(3):20–23, 1996.

[11] R. Romero, L. Feletti, C. Re, and A. Mariscotti. Opera 2015 project: accurate measurement equipment for earthquake electromagnetic emissions and radio seismic indicator. *Sensors*, 23(5):2379, 2023.

[12] H. W. Silver, editor. *The ARRL Handbook for Radio Communications 2022*. The American Radio Relay League, Inc., 2021.

[13] Vishay Siliconix. *Power MOSFET IRF9610*, 2021. Document Number: 91080.